 doi:10.20944/preprints202011.0492.v1

Article

Direct and Label-Free Monitoring of Albumin in 2D Fatty Liver Disease Model using Plasmonic Nanogratings.

Gerardo A. Lopez-Muñoz [1], Ma. Alejandra Ortega [1], Ainhoa Ferret-Miñana [1], Francesco De Chiara [1] and Javier Ramón-Azcón [1,*]

[1] Institute for Bioengineering of Catalonia (IBEC), The Barcelona Institute of Science and Technology, Baldiri I Reixac, 10-12, Barcelona, Spain; glopez@ibecbarcelona.eu (G.A.L.M); mortega@ibecbarcelona.eu (M.A.O.); aferret@ibecbarcelona.eu (A.F.M.); fdechiara@ibecbarcelona.eu (F.D.C.)

* Correspondence: jramon@ibecbarcelona.eu; Tel.: (+34-934-039-735)

Abstract: Non-alcoholic fatty liver (NAFLD) is a metabolic disorder related with a chronic lipid accumulation within the hepatocytes. This disease is the most common liver disorder worldwide and it is estimated that is present in up to 25% of the world's population. However, the real prevalence of this disease and the associated disorders is unknown mainly because reliable and applicable diagnostic tools are lacking. It is known that the level of albumin, a pleiotropic protein synthetized by hepatocytes, is correlated with the correct function of the liver. The development of a complementary tool that allow the direct, sensitive, and label-free monitoring of albumin secretion in hepatocyte cell culture can provide insight about the mechanism and drugs action in NAFLD. With this aim, we have developed a simple integrated plasmonic biosensor based on gold nanogratings from periodic nanostructures present in commercial Blu-ray optical disc. This sensor allows the direct and label-free monitoring of albumin in a 2D fatty liver disease model under flow conditions using highly specific polyclonal antibody. This technology avoids both the amplification and blocking steps showing a limit of detection within pM range (≈ 0.39 ng/mL). Thanks to this technology, we identified the optimal fetal bovine serum (FBS) concentration to maximize the lipid accumulation within the cells. Moreover, we discovered that at third day from lipids challenge, the hepatocytes increased the amount of albumin secreted. These data demonstrate the ability of hepatocytes to respond to the lipid stimulation releasing more albumin. Further investigation needed to unveil the biological significance of that cell behaviour.

Keywords: 2D fatty liver in vitro model; Blu-Ray disc; Plasmonic Nanomaterials; Label-Free Biosensing

1. Introduction

The chronic accumulation of fat within the liver, known as non-alcoholic fatty liver (NAFL), increased exponentially in last 10 years. Over 25% of the global population is affected by NAFL although it is underdiagnosed [1]. This tremendous upsurge in NAFL disease (NAFLD) prevalence is related with the increase in consumption of ultra-processed low-cost food and a dramatic decline in physical activity over the last years. NAFL range from simple steatosis, where >5% of the liver cells contain lipid droplets, to its more aggressive form the non-alcoholic steatohepatitis (NASH) characterized by liver inflammation. The gold standard for the detection of NAFLD is the biopsy where a trained pathologist scores the stage of the disease [2].

The steatotic hepatocytes (the main cell type of the liver) have altered cell metabolic capacity and plasticity that lead to a more vulnerable liver to further injuries such as infection and oxidative stress [3]. Moreover, there is no way to detect the early stage of hepatocytes response to the chronic lipid accumulation, therefore the molecular mechanism(s) that underlie the steatosis remain unveiled. Understanding how the hepatocytes metabolism changes from healthy to disease status is of primary importance for the design of more precise therapeutic intervention.

Preprints (www.preprints.org) | NOT PEER-REVIEWED | Posted: 19 November 2020 doi:10.20944/preprints202011.0492.v1

Albumin (ALB) is a transport globular protein synthesized in the liver by hepatocytes and released into the bloodstream. ALB participates in many functions within the body such as regulating the oncotic pressure and boosting the immune system. Also, it functions as carrier of a variety of compounds such as hormones, steroids, drugs, and fatty acids. The level of albumin in healthy human varies from 3.5 g/dL to 5 g/dL and it represents up to the 50% of the total plasma protein content [4]. Finally, the monitoring of ALB levels has an enormous clinical relevance because its level is correlated with the functionality of the liver. In fact, the levels of serum ALB in malnourished people and patients with liver damage are dramatically reduced with the progression of the disease.

Cell culture offers a simple and low-cost functional test to study the response of the cells to the lipid challenge. It is a widely used in vitro tool that can contribute to our understanding of cell biology, mechanisms of diseases, drug action, and protein/biomarkers production [5]. Cell culture integration with lab-on-a-chip devices would offer significant advantage in monitoring the real-time release of potential biomarkers. Optical biosensors are ideal candidates for those kind of applications because of their label-free detection of multiple analytes with high sensitivity while avoiding unnecessary sample pretreatments [6].

Recently a simple and cost-effective fabrication method to develop optical biosensors based on plasmonic nanogratings has been demonstrated [7]. This approach is based on industrially produced Blu-ray discs as a nanograting-containing substrate and it allows the possibility to generate plasmonic effects in the visible range when incorporating gold layer films with thicknesses in the range of 50-100 nm with a high degree of reproducibility, and simple and low-cost fabrication while achieving biosensing performance similar to those obtained with similar engineered nanostructures [8,9].

Based on these considerations we have developed a nanostructured plasmonic sensor based on commercial Blu-ray discs with integrated microfluidics for sensitive detection of albumin in cell culture supernatant from 2D fatty liver disease model (See graphical abstract in Figure 1). The gold nanograting-based plasmonic sensors were fabricated following a simple and reproducible fabrication process, where a direct immunoassay detection has been implemented. This approach allows direct and label-free monitoring of proteins of interest while avoiding the use of incubation or washing steps, and any other sample pretreatment.

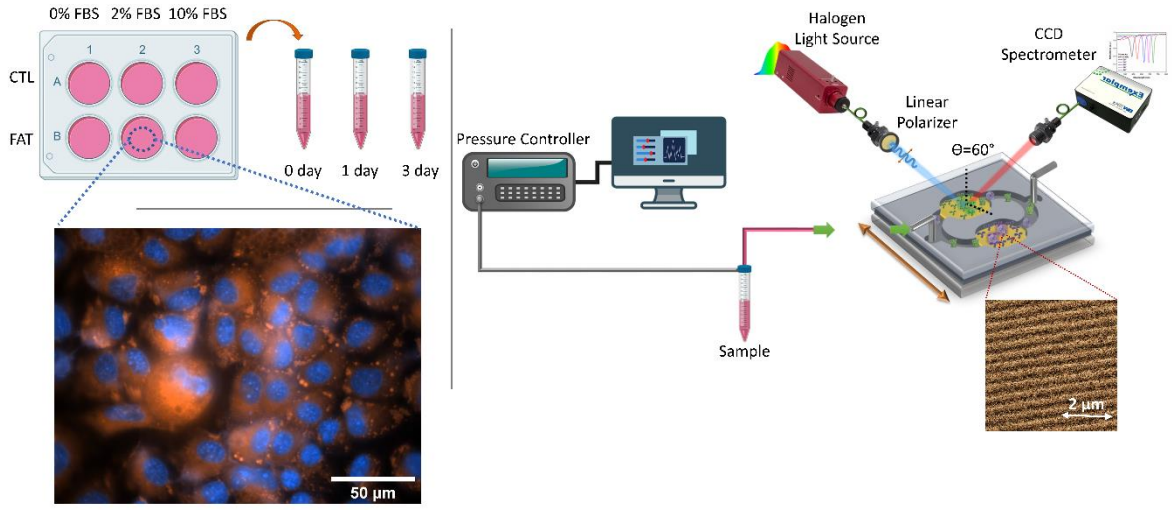

Figure 1. Schematic representation for the development of a high throughput plasmonic sensing platform for monitoring of albumin levels in 2D *in vitro* model of Fatty Liver disease.

Preprints (www.preprints.org) | NOT PEER-REVIEWED | Posted: 19 November 2020 doi:10.20944/preprints202011.0492.v1

2. Materials and Methods

2.1. Development of the in vitro Fatty liver disease model

The **cells** employed for this study are healthy immortalized mouse hepatocytes purchased from ATCC® AML12 (CRL-2254™, VI, USA). They were kept in DMEM:F12 Medium (ATCC 30-2006) supplemented with 10% fetal bovine serum (FBS; ATCC 30-2020), 10 µg/mL insulin, 5.5 µg/mL transferrin, 5 ng/ml selenium (41400045, Life Technologies S.A., MD, USA), 40 ng/mL dexamethasone (D4902, Merk, FS, Switzerland). For each experiment, the cells were seeded at density of 26 000/cm^2 and cultured at 37°C, 5% CO_2.

Non-esterified fatty acids (NEFAs) solution is prepared dissolving oleic acid (OA, O1008-1G, Merk, FS, Switzerland) and Palmitic acid (PA, P0500-10G, Merk, FS, Switzerland) in PBS with bovine serum (1%) at ratio OA/PA 1:2. The final concentration testes is 400 µM.

Cell metabolism is measured using the CellTiter 96® AQueous One Solution Cell Proliferation Assay (G3582, Promega, AM, Switzerland). Briefly, at day 1 and day 3, the supernatant was removed, and cells washed twice with PBS. After that, 100 µL of fresh medium plus 20 µL of MTS was added and incubated for 3 hours. The absorbance was recorded at 490 nm.

Cell viability was assessed by alamarBlue™ Cell Viability Reagent (DAL1025, Thermo Fisher Scientific, Spain). At indicated timepoints, the supernatant was removed, and cells washed twice with PBS. After that, 90 µL of fresh medium plus 10 µL of alamarBlue™ reagent for 3 hours. The fluorescence signal was recorded using Ex(530 nm)/Em(590 nm).

The intracellular lipid uptake was observed using adipored™ (PT-7009, Lonza, MD, USA) using fluorescence microscopy Ex(485 nm)/Em(535 nm) while the signal was recorded using spectrophotometer with same Ex/Em wavelength. The intracellular level of albumin was assessed by immunocytochemistry. The cells were seeded onto µ-Slide 8 Well (80826, Ibidi, Germany) for the indicated length of the experiments. At day of the essay, the cells were washed twice with PBS. Following, they were fixed using 4% paraformaldehyde - PBS at room temperature for 10 minutes. The permeabilization was obtained using a 0.5% Triton X-100 in PBS solution at room temperature (RT) for 5 minutes. The blocking was done using 2% horse serum in PBS for 1 hour at RT. The albumin antibody (GTX102419, GeneTex, IR, USA) was diluted 1:200 in 1% horse serum solution and incubated over night at 4 degrees. The day after, the excess of the antibody was washed away with PBS, the cells were then incubated with a goat anti-Mouse (A28175, Thermo Fisher, USA) diluted 1:2000 in PBS in 1% horse serum solution. DAPI was also added at 1:1000 concentration for 1 hour at RT. The cells were washed again with PBS and mounted with Fluoromount-G™ (00-4958-02, Thermo Fisher, USA).

2.2. Fabrication and integration of the nanoplasmonic chip

Single layer recordable Blu-ray discs (43743, Verbatim, Taiwan) were used after removal of their protective and reflective films. These were removed by cutting the disc in individual plasmonic chips (size 8.5 cm2) and then by immersing it in a hydrochloric acid solution (2M HCl) overnight. After rinsing with deionized water and nitrogen drying of the substrate, an 80 nm thick layer of gold was deposited by resistive thermal evaporation (1 Å/s). A microfluidic flow cell for carrying out the biodetection in solution was developed using a patterned microfluidic channel in a 140 µm thick double-sided adhesive tape sheet (Mcs-foil-008, Microfluidic ChipShop GmbH, Germany). The proposed design integrates a microfluidic splitter on chip that allow duplicated biodetection of one protein target or multiplexed biodetection of two protein targets in parallel. A 2 mm tick patterned polymethyl methacrylate (PMMA) lid was added as a cover to facilitate the connection of the fluidic tubes.

2.3. Experimental Optical Setup and FDTD Simulations

The integrated sensor chips were clamped to a custom-made optical platform for reflectance measurements. The chips were connected to a microfluidic pressure pump (OB1 Mark I, Elveflow, France), with adjustable pumping speed guaranteeing a constant liquid flow. Reflectance

Preprints (www.preprints.org) | NOT PEER-REVIEWED | Posted: 19 November 2020 doi:10.20944/preprints202011.0492.v1

measurements were performed under TM-polarization of a compact stabilized broadband light source (SLS201L, Thorlabs, Germany) at 60°. The incident excitation plane was perpendicularly aligned to the nanograting direction. The reflected light was collected, and fiber coupled to a compact Charge-Coupled Device (CCD) spectrometer (Exemplar UV-NIR, BWTek, Germany).

Reflectivity spectra were acquired every 1 ms and 50 consecutive spectra were measured and averaged to provide the final spectrum. These acquisition parameters were selected to obtain optimum signal to noise (S/N) ratio without significantly increasing the data acquisition time. Changes in the resonance peak position (λSPR) were tracked via centroid determination by peak analysis using Origin 2018 software (OriginPro, OriginLab Co., USA). Reflection spectra were collected in water (n=1.33 RIU) and solutions of glucose in water (ranging between 1.337 and 1.368 RIU) to determine the bulk sensitivity of the plasmonic nanograting sensor.

Three-dimensional FDTD simulations were performed using commercial software (FTDT solution, Lumerical Inc., Canada). Structural parameters of the Blu-ray discs based on Atomic Force used in the simulations (i.e., a grating period of 320 nm, grating width of 100 nm and a height of 20 nm) were according to Atomic Force Microscopy (AFM) images from previous results [10]. Periodic boundary conditions were used in x and y axis, and perfect matched layers (PML) approach was used in the z axis, with a uniform mesh size of 2 nm in all axis. The FDTD simulations were performed in the range from 400 nm to 1000 nm, under TM-polarized light with an oblique light incidence angle of 60°.

2.4. Surface biofunctionalization of nanoplasmonic sensing platform

Alkanethiol for self-assembled monolayer (SAM) formation (11-mercaptoundecanoic acid, MUA), (1- ethyl-4 (3-dimethylaminopropyl) carbodiimide hydrochloride (EDC) and sulfo-N hydroxysuccinimide (s-NHS) for carboxylic groups activation and ethanolamine were acquired to Sigma Aldrich (Germany). Sensor chips were cleaned and activated for surface functionalization by performing consecutive rising with ethanol and deionized water, drying with N2 stream and finally by placing them in a UV ozone generator (BioForce Nanoscience, USA) for 20 min. An alkanethiol self-assembled monolayer (SAM) with reactive carboxylic groups was obtained by coating the sensor chip with 2.5 mM MUA in ethanol overnight at room temperature. Then, the surface was rinsed with ethanol and carefully washed with MES buffer.

The immobilization of the Mouse Serum Albumin antibody (MSA) was performed ex situ following the protocol previous described by Acimovic-Ortega et al. [11]. For the activation of the carboxylic groups a solution of 0.2 M EDC/0.05 M sulfo-NHS in (2-ethanesulfonic acid) MES buffer (25 mM pH 5.7) was dropped over the SAM monolayer for 40 min. After washing steps using MES buffer, 50 μg/mL of MSA antibody solution in (phosphate buffer) PB (10 mM pH 7.4) was dropped for 120 min. Finally, sensor was submerged on an ethanolamine solution 50 μg/mL prepared in PB 10 mM pH 7.2 for 15 min to block unreacted remaining active carboxylic groups. Chips were carefully dried with a N2 stream and bonded to the microfluidics channels and finally placed in the optical platform and filled with PB for optimization and assessment studies, different concentrations of MSA protein diluted in Phosphate Buffer Saline 10 mM pH 7.2 (PBS) were flowed over the functionalized surface at 80 μL/min. Calibration curves were fitted to a one-site specific binding model. Data points for each concentration were collected 30 min after injection. Albumin from mouse serum (A-3139t, Merck, Germany) was used as standard protein for preparation of calibration curves at different FBS content and sensor optimization.

3. Results and Discussion

3.1. In vitro fatty liver disease model

To reproduce some of the features of NAFLD in vitro, we first prepared the lipid solution (Non-esterified fatty acids – NEFAs) dissolving oleic and palmitic acids in a solution of bovine serum and phosphate buffer saline (PBS) because of their insolubility in water solutions as previously published [12]. Second, we challenged the hepatocytes with a lipid solution concentrated 400 μM at 0, 1 and 3

Preprints (www.preprints.org) | NOT PEER-REVIEWED | Posted: 19 November 2020 doi:10.20944/preprints202011.0492.v1

days using 0%, 2% and 10% of FBS in order to see which of those conditions accumulate the highest concentration of lipid without affecting greatly the cell viability (Figure 1a). From day 1, all the experimental conditions displayed lipid accumulation using bright microscopy (black arrow, Figure 1b). To assess cell viability and metabolism, we employed two tests: the MTS (absorbance) and Alamarblue™ (fluorescence), respectively. Both assays showed an increase in cell number and metabolism from day 1 (D1) to day 3 (D3) in the untreated conditions cultured in presence of different concentration of FBS (Figure 1c). However, cells cultured in 0% FBS showed a smaller increment over time compared with FBS 2%, while FBS 10% showed the highest increment. Those tests also revealed a significative reduction in viability and metabolism of cells upon lipid exposure in all the conditions under investigation (Figure 1c). The lipid accumulation within the cells was assessed using Adipored assay (Figure 1d). The AdipoRed™ becomes fluorescent when it is stored in an hydrophobic enviroment like a cell membrane that contains double-layer of lipids and fat droplets. All the conditions under investigation exhibit a significative accumulation of AdipoRed™ upon treatment with NEFAs solution compared with untreated condition, regardless from the cell number and metabolism (white arrows, Figure 1d). Interestingly, starved cells (FBS 0%), did not shown almost any fat accumulation upon treatment. Taken together, these data show that the fat exposition induces a reduction in hepatocytes viability and metabolism while intracellular lipid accumulation. Both are features of the NAFLD liver.

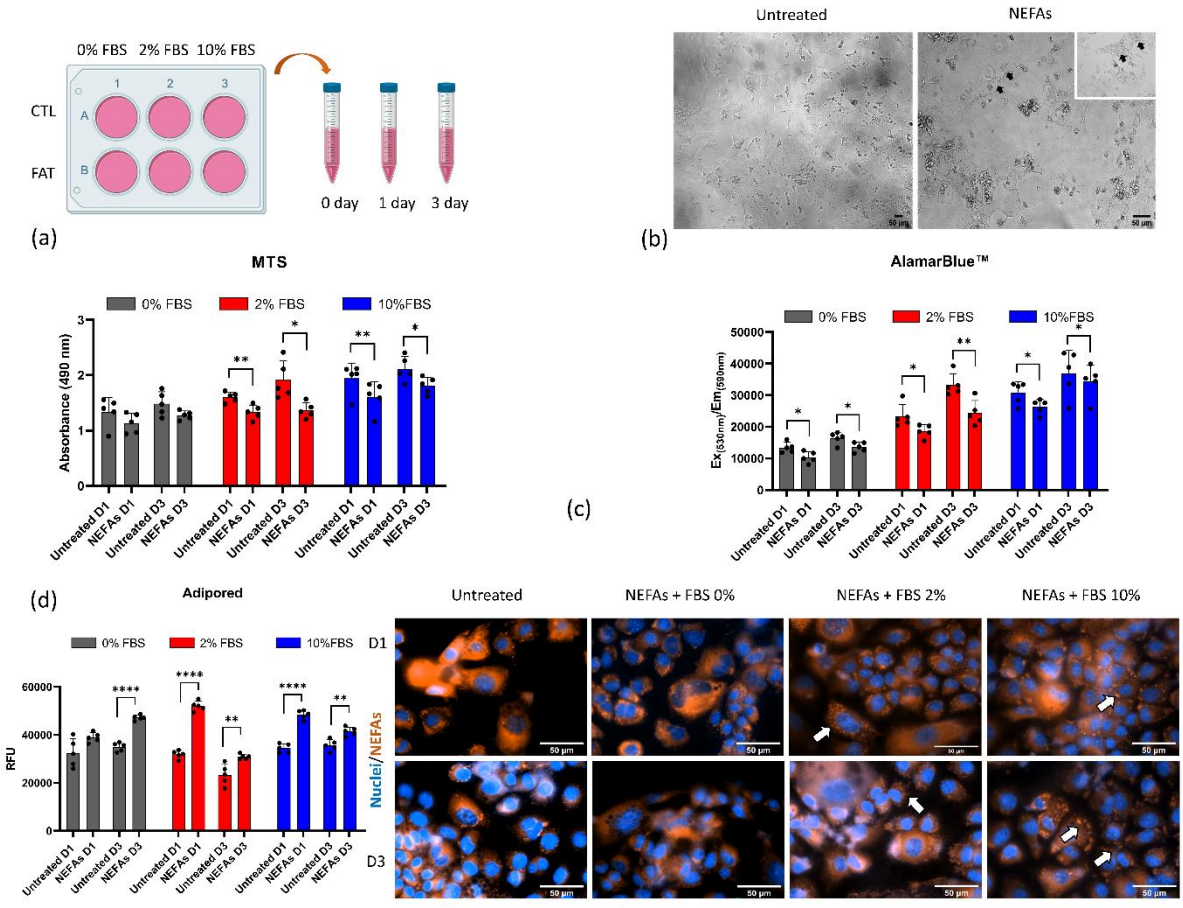

Figure 2. In vitro model of fatty hepatocytes. (a) experimental set up. (b) Bright microscopy of mouse hepatocytes with and without treatment with non-esterified fatty acids. (c) Cell viability and metabolism of hepatocytes treated with 400 μM of NEFAs up to 3 days. (d) Quantitative and qualitative intracellular fat accumulation using Adipored™ assay.

Preprints (www.preprints.org) | NOT PEER-REVIEWED | Posted: 19 November 2020 doi:10.20944/preprints202011.0492.v1

3.2. Simulation and Characterization of nanoplasmonic sensor.

Gold coated nanogratings were fabricated taking advantage of the precise and large area of nanostructured arrays present in commercial Blu-ray discs. As showed in Figure 3a, there is a good agreement between the FDTD calculated and the experimental reflectance spectra. The differences in the resonance peaks position between the simulated and fabricated nanograting are mainly due to unavoidable geometrical and metallic layer imperfections. The FDTD electric field distribution for an 80 nm gold coated nanograting (Figure 3b) under a 60° angle of incidence of light shows a minimal interaction of plasmons with the underlying substrate, it results in a high intensity and long decay length of the electric field over the sensing media due to the generation of surface lattice resonances as previously reported [7]. Considering the performance of the sensors, a bulk sensitivity of ≈ 392 nm/RIU (Figures 3c and 3d) is achieved which is highly competitive and similar to those obtained with engineered nanoslits/nanogratings sensors making them interesting for the development of cost-effective biosensor devices.

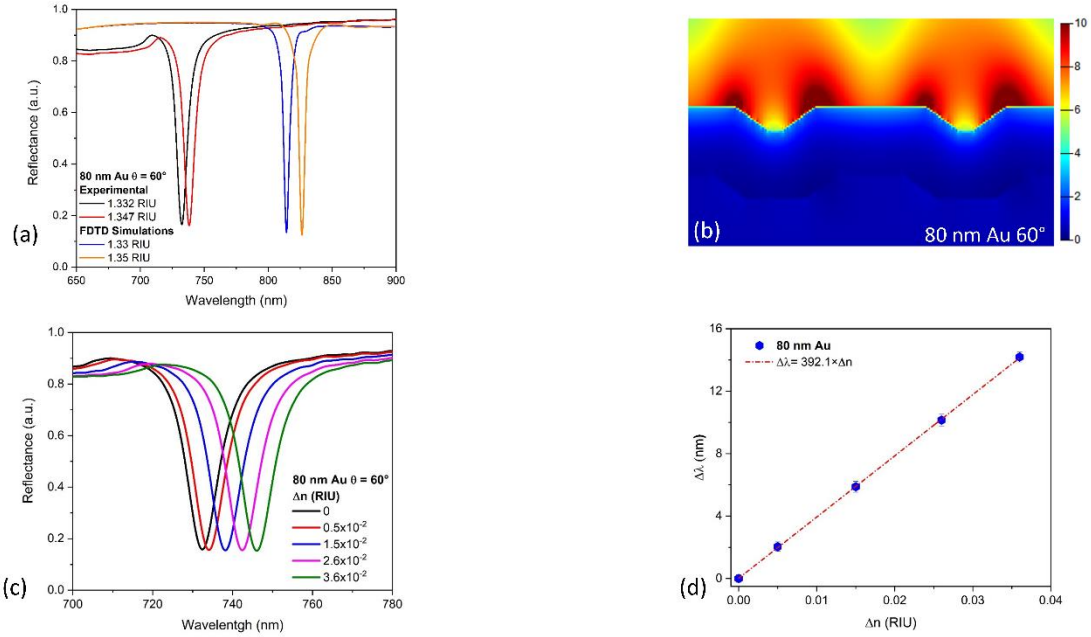

Figure 3. FDTD Simulations of the proposed sensor and sensing performance evaluation. (a) Experimental and simulated optical reflectance spectra under TM-polarization with a light incident angle of 60° for the nanostructured plasmonic sensor fabricated. (b) Simulated electric field distribution for the 80 nm gold thickness layer on the polycarbonate nanograting under TM-polarization for a light incidence angle of 60°. (c) Displacement of the reflectance spectra for the plasmonic nanogratings based sensor fabricated with different refractive index solutions based on ethanol-water mixtures. (d) Calibration curve and bulk sensitivity determination for the 80 nm gold thickness layer sensor at a light incidence angle of 60°.

3.3. Albumin detection by the nanoplasmonic sensing integrated platform

Once nanoplasmonic sensors were fabricated, the MSA was anchored to the gold surface to perform a selective detection of albumin via self-assembled monolayer formation. After the ex-situ biofunctionalization, connection with the PMMA microfludics cover was performed. Figure 4a shows the nanostructured plasmonic biosensor integrated the microfluidic splitter on chip, this design simplifies the microfluidic instrumentation and, if required, a multiplexed measurement (either the biodetection of two biomarkers or the replica of a measurement of a single biomarker). The insert in the Figure 4a shows a scanning electron microscopy (SEM) image of the fabricated gold nanogratings with a high reproducibility in a large scale as result of industrial manufacturing. In figure 4b, the

Preprints (www.preprints.org) | NOT PEER-REVIEWED | Posted: 19 November 2020 doi:10.20944/preprints202011.0492.v1

nanoplasmonic sensor connected to the microfluidic system in reflectance mode experimental set-up and clamped to a motorized linear stage to move between the sensing areas.

Optimization of the capture antibody concentration is shown in figure 4c. Black line correspond to SPR shift for MSA antibody at different concentration after the ex situ biofunctionalization protocol. 10, 20, 50 and 100 µg/mL was evaluated obtaining a saturation plateau for concentration up to 20 µg/mL. Nevertheless, in order to evaluate the capability of the detection for the anchored antibody layers it was flowed 1µg/mL albumin protein solution. In figure 4c (red line graph) we can observe that maximum SPR shift signal is obtained for 50 µg/mL MSA concentration, which we assume as optimal concentration for further experiments.

Calibration curves were performed using serial dilutions of commercial albumin 0.1, 1, 10, 200, 1000 and 5000 ng/mL diluted in cell media containing FBS at 0, 2 and 10%. Before flowing protein solutions, cell media without albumin was used to set a baseline, subtracting the possible matrix effects. In figure A1, it can be observed the native SPR peak and shift generated by increment of albumin concentration using an additive assay.

Curves were fitted to a four-parameter equation according to the following formula: Y = [(A - B)/1 - (x/C)D] + B, where A is the maximal signal, B is the minimum, C is the concentration producing 50% of the maximal signal, and D is the slope at the inflection point of the sigmoid curve. The calculation of the limit of detection (LOD) and the limit of quantification (LOQ) was based on ELISA methodology [13]. For a standard curve, the LOD is considered as the concentration corresponding to the interpolated intersection of the 10% confidence interval of the lower asymptote with the four-parameter equation fit of standards data. In figure 4d, it is shown the calibration curve performed in cell media containing 2% FBS. After analysis we obtained a LOD of 0.39 ng/mL. Calibration curves using 0 and 10% FBS are shown in Figure A2, obtaining LOD of 0.36 and 0.37 ng/mL respectively. We can observe that FBS content do not have a direct effect on albumin detection. Experiments were performed with a total of 2 replicates. Those calibration curves were used later during quantification assays for unknow samples generated from the in vitro system. As previously reported by López-Muñoz et al. (2017, *Biosens. Bioelectron.*) it is possible to achieve nanoplasmonic sensors with a coefficient of variation below 1% in their optical performance with this fabrication process which demonstrate the high reproducibility between the sensors.

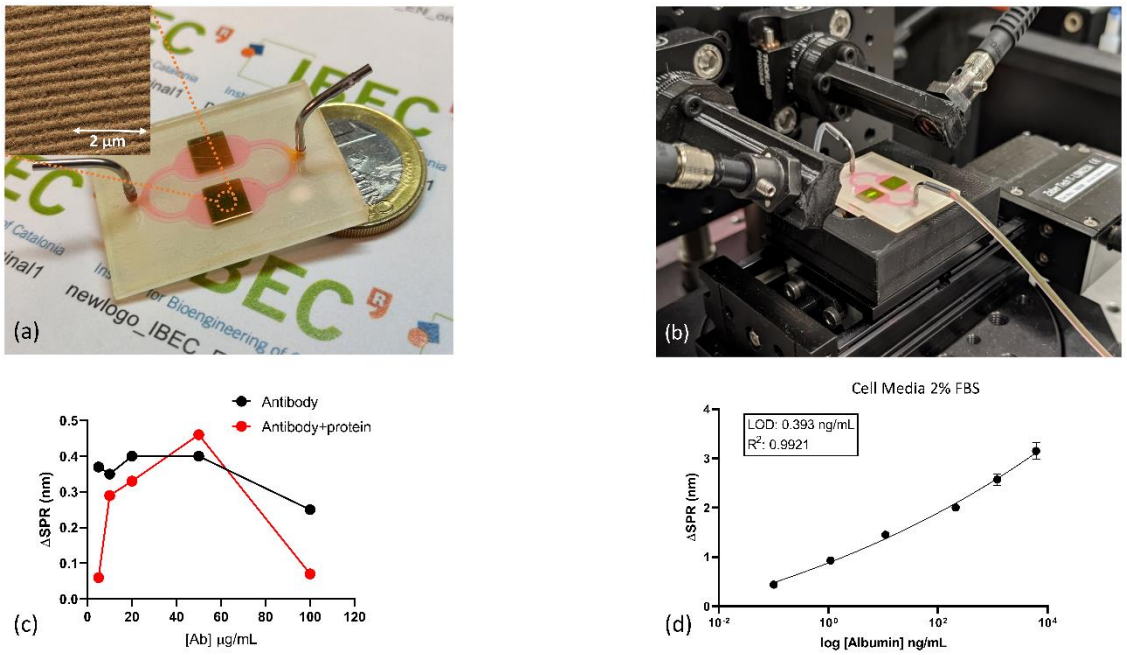

Figure 4. Experimental set-up and optimization of biosensing assay. (a)Photograph of the 2-channel packed sensor. The insert shows a SEM photograph of the fabricated gold plasmonic nanogratings. (b) Photograph of the experimental system. c) Mouse serum albumin (capture antibody) optimization. Red line corresponds to SPR shift obtained by changing the MSA concentration on functionalized

Preprints (www.preprints.org) | NOT PEER-REVIEWED | Posted: 19 November 2020 doi:10.20944/preprints202011.0492.v1

nanoplasmonic surface; Red line correspond to SPR shift obtained after evaluating detection of 1µg/mL at the previous MSA concentrations anchored on sensors surface (d) calibration curve of albumin detection performed in DMEM cell media containing 2%FBS. LOD of 0.393 ng/mL was obtained.

Detection of secreted albumin from the in vitro model of fatty liver was performed under fluidic conditions. Supernatants of controls and fatty liver was collected at day 0, 1 and 3. Each sample was interrogated by an individual 2-channel nanoplasmonic sensing platforms and later fitted from the corresponding calibration curve for quantification. Figure 5a shows the albumin secretion profile from untreated and fatty hepatocytes for all the conditions. The albumin concentration increases more significantly in the 2% FBS condition compared to the control. Nevertheless, the albumin secretion remains constant at FBS content of 0 and 10%. In case of 2% FBS condition, we evaluate independently albumin secretion of samples in cell media with and without fat to confirm that increment of signal is a selective detection of the protein without added effect from the fat supplement or media supplements (Figure 5b). We validated the data obtained from the sensors with the level of intracellular albumin by immunocytochemistry (Figure 5c). The cells grown more in presence of FBS 10% than the cells with other two FBS content, however they secreted less albumin compared with the other two, especially the FBS 2%. The cells seem to find optimal a starving environment with FBS 2% for albumin production because allow them to differentiate more compared to the other two conditions.

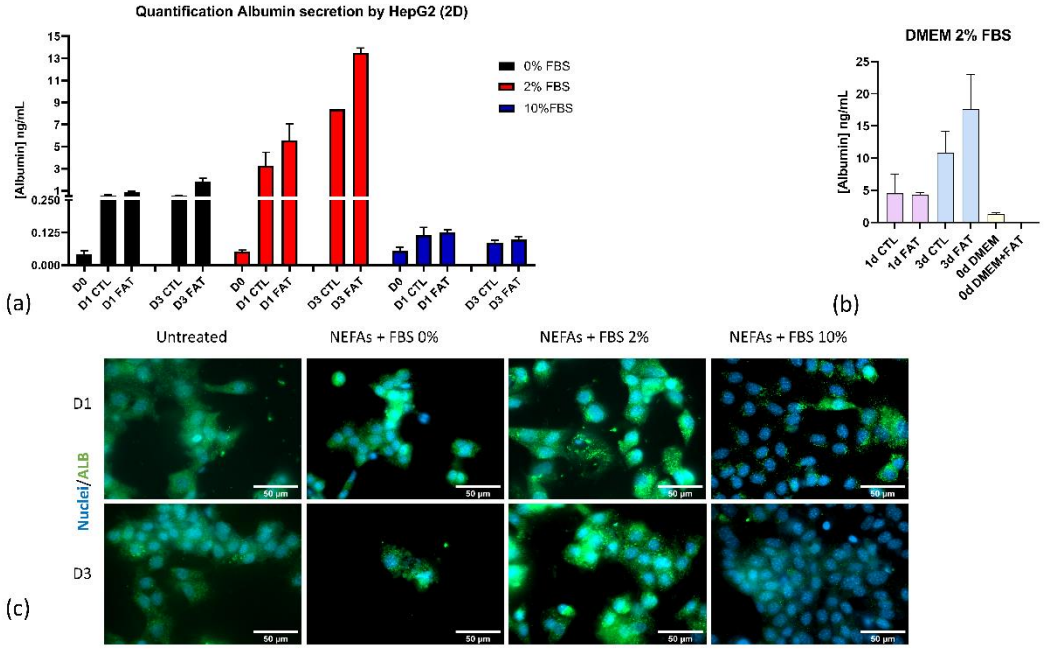

Figure 5. Compairson biodetection of albuming by nanoplasmonic biosensor and fluorescense assay. (a) Quantification of secreted albumin generated by 2D in vitro model of fatty hepatocytes treated with cell media at 0, 2 and 10% FBS during 3 days. (b) Evaluation of matrix effect and fat supplement in the cell media with the detection of secreted albumin performed in cell media at 2% FBS. (c) Intracellular staining of albumin using immunocytchemistry technique.

5. Conclusions

The in vitro data herein presented reflect both the phenotypical and functional changes that take place in fatty hepatocytes in vivo. In fact, the ´´viability and metabolic activity decrease upon challenge with NEFAs while the albumin production increase as consequence of adaptation to the new environment. The simple label-free integrated plasmonic biosensor based on Blu-ray discs nanogratings allowed us to monitor albumin secretion over time in an in vitro fatty liver model. This represent a useful tool to study the evolution of the disease in vitro. Moreover, we took advantage of

the cost-effective Blu-ray disc to achieve the fabrication of high throughput sensors. This prototype is totally customizable, and it has been employed as a multi-analyte detection system in cell culture supernatant media, with a LOD in the pM order without any amplification or pretreatment of the sample. Due to its high versatility and the straightforward integration in lab-on-a-chip devices, the presented plasmonic nanomaterial is a promising candidate for the development of monitoring platforms for cell cultures.

Author Contributions: G.A.L.M., M.A.O., F.D.C. and J.R.A. conceptualized the experiments. A.F.M. and F.D.C. developed the 2D cell cultures and collected the samples. G.A.L.M. designed and fabricated the plasmonic nanogratings. M.A.O. carried out the optimization and implementation of biofunctionalization protocol on sensors and G.A.L.M performed the plasmonic measurements. G.A.L.M., M.A.O., F.D.C. and J.R.A. wrote the presented paper. G.A.L.M., M.A.O., F.D.C. A.F.M. and J.R.A. took a part in the discussion and conclusion of the following manuscript. All authors have read and agreed to the published version of the manuscript.

Funding: This project received financial support from the European Research Council program under grants ERC-StG-DAMOC (714317), the Spanish Ministry of Economy and Competitiveness, through the "Severo Ochoa" Program for Centres of Excellence in R&D (SEV-2016-2019) and "Retos de investigación: Proyectos I+D+i" (TEC2017-83716-C2-2-R), the CERCA Programme/Generalitat de Catalunya (2014-SGR-1460) and Fundación Bancaria "la Caixa"- Obra Social "la Caixa" (project IBEC-La Caixa Healthy Ageing) to JR-A. G.A.L.M. was supported by a postdoctoral fellowship SECTEI (Secretaria de Educación, Ciencia, Tecnología e Innovación de la Ciudad de México) SECTEI/143/2019 and CM-SECTEI/137/2020.

Acknowledgments: G.A.L.M. acknowledge SECTEI (Secretaria de Educación, Ciencia, Tecnología e Innovación de la Ciudad de México) for Postdoctoral Fellowship SECTEI/143/2019 and CM-SECTEI/137/2020.

Conflicts of Interest: The authors declare no conflict of interest.

References

1. Younossi, Z.M.; Koenig, A.B.; Abdelatif, D.; Fazel, Y.; Henry, L.; Wymer, M. Global epidemiology of nonalcoholic fatty liver disease—Meta-analytic assessment of prevalence, incidence, and outcomes. *Hepatology* **2016**, doi:10.1002/hep.28431.
2. Bedossa, P. Diagnosis of non-alcoholic fatty liver disease/non-alcoholic steatohepatitis: Why liver biopsy is essential. *Liver Int.* **2018**, doi:10.1111/liv.13653
3. De Chiara, F.; Checcllo, C.U.; Azcón, J.R. High protein diet and metabolic plasticity in non-alcoholic fatty liver disease: Myths and truths. *Nutrients* **2019**, doi:10.3390/nu11122985
4. Sun, L.; Yin, H.; Liu, M.; Xu, G.; Zhou, X.; Ge, P.; Yang, H.; Mao, Y. Impaired albumin function: a novel potential indicator for liver function damage? *Ann. Med.* **2019**, doi: 10.1080/07853890.2019.1693056
5. Kapałczyńska, M.; Kolenda, T.; Przybyła, W.; Zajączkowska, M.; Teresiak, A.; Filas, V.; Ibbs, M.; Bliźniak, R.; Łuczewski, Ł.; Lamperska, K. 2D and 3D cell cultures – a comparison of different types of cancer cell cultures. *Arch. Med. Sci.* **2018**, doi:10.5114/aoms.2016.63743.
6. Lopez, G.A.; Estevez, M.C.; Soler, M.; Lechuga, L.M. Recent advances in nanoplasmonic biosensors: Applications and lab-on-a-chip integration. *Nanophotonics* **2017**, doi:10.1515/nanoph-2016-0101
7. López-Muñoz, G.A.; Estevez, M.C.; Peláez-Gutierrez, E.C.; Homs-Corbera, A.; García-Hernandez, M.C.; Imbaud, J.I.; Lechuga, L.M. A label-free nanostructured plasmonic biosensor based on Blu-ray discs with integrated microfluidics for sensitive biodetection. *Biosens. Bioelectron.* **2017**, doi:10.1016/j.bios.2017.05.020.
8. Wi, J.S.; Lee, S.; Lee, S.H.; Oh, D.K.; Lee, K.T.; Park, I.; Kwak, M.K.; Ok, J.G. Facile three-dimensional nanoarchitecturing of double-bent gold strips on roll-to-roll nanoimprinted transparent nanogratings for flexible and scalable plasmonic sensors. *Nanoscale* **2017**, doi:10.1039/c6nr08387k.
9. Lee, K.L.; Hsu, H.Y.; You, M.L.; Chang, C.C.; Pan, M.Y.; Shi, X.; Ueno, K.; Misawa, H.; Wei, P.K. Highly Sensitive Aluminum-Based Biosensors using Tailorable Fano Resonances in Capped Nanostructures. *Sci. Rep.* **2017**, doi:10.1038/srep44104.
10. López-Muñoz, G.A.; Estévez, M.C.; Vázquez-García, M.; Berenguel-Alonso, M.; Alonso-Chamarro, J.; Homs-Corbera, A.; Lechuga, L.M. Gold/silver/gold trilayer films on nanostructured polycarbonate substrates for direct and label-free nanoplasmonic biosensing. *J. Biophotonics* **2018**, doi: 10.1002/jbio.201800043

11. Aćimović, S.S.; Ortega, M.A.; Sanz, V.; Berthelot, J.; Garcia-Cordero, J.L.; Renger, J.; Maerkl, S.J.; Kreuzer, M.P.; Quidant, R. LSPR chip for parallel, rapid, and sensitive detection of cancer markers in serum. *Nano Lett.* **2014**, doi:10.1021/nl500574n.
12. De Chiara, F.; Heebøll, S.; Marrone, G.; Montoliu, C.; Hamilton-Dutoit, S.; Ferrandez, A.; Andreola, F.; Rombouts, K.; Grønbæk, H.; Felipo, V.; et al. Urea cycle dysregulation in non-alcoholic fatty liver disease. *J. Hepatol.* **2018**, doi:10.1016/j.jhep.2018.06.023.
13. Estévez, M.-C.; Font, H.; Nichkova, M.; Salvador, J.-P.; Varela, B.; Sánchez-Baeza, F.; Marco, M.-P. Immunochemical Determination of Pharmaceuticals and Personal Care Products as Emerging Pollutants BT - Water Pollution: Emerging Organic Pollution in Waste Waters and Sludge, Vol. 2. In; Barceló, D., Ed.; Springer Berlin Heidelberg: Berlin, Heidelberg, 2005; pp. 181–244 ISBN 978-3-540-31493-6.

Preprints (www.preprints.org) | NOT PEER-REVIEWED | Posted: 19 November 2020 doi:10.20944/preprints202011.0492.v1

Appendix A. Supplementary Figures

A1

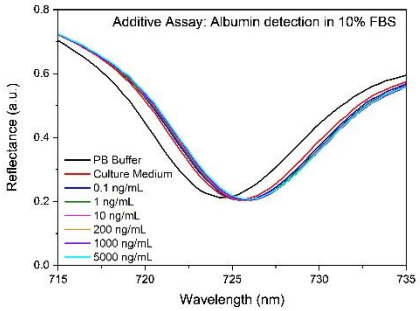

A2